Environmental Science Nano

PAPER

View Article Online
View Journal | View Issue

Cite this: *Environ. Sci.: Nano*, 2014, **1**, 248

Tracking dissolution of silver nanoparticles at environmentally relevant concentrations in laboratory, natural, and processed waters using single particle ICP-MS (spICP-MS)†

D. M. Mitrano,[ab] J. F. Ranville,[a] A. Bednar,[c] K. Kazor,[d] A. S. Hering[d] and C. P. Higgins*[e]

The interplay between engineered nanoparticle (ENP) size, surface area, and dissolution rate is critical in predicting ENP environmental behavior. Single particle inductively coupled plasma mass spectrometry (spICP-MS) enables the study of ENPs at dilute (ng L^{-1}) concentrations, facilitating the measurement of ENP behavior in natural systems. Here, the utility of using spICP-MS to quantitatively track the changes in particle diameter over time for 60 and 100 nm Ag ENPs (citrate, tannic acid, and polyvinylpyrrolidone coated) was demonstrated. Short term (<24 h) and intermediate term (1 week) dissolution was examined, with rates for all particles slowing by over an order of magnitude after approximately 24 h. Dissolution was measured primarily as a decrease in particle diameter over time but direct measurement of $Ag^{+}_{(aq)}$ was also completed for the experiments. The importance of water chemistry including chloride, sulfide, and dissolved organic carbon (DOC) was demonstrated, with higher concentrations (1 mg L^{-1} Cl^{-}, S^{2-} and 20 mg L^{-1} DOC) resulting in negligible Ag ENP dissolution over 24 h. Slight decreases in particle diameter (<10%) were observed with lower concentrations of these parameters (stoichiometric Cl^{-}, S^{2-} and 2 mg L^{-1} DOC). Capping agents showed variable effects on dissolution. ENP behavior was also investigated in natural (moderately hard water, creek water) and tap water. Water chemistry was the most significant factor affecting dissolution. Near complete dissolution was observed in chlorinated tap water within several hours. Though modeled as first-order kinetic transformations, the dissolution rates observed suggested the dissolution kinetics might be significantly more complex. Two specific highlights of the benefits of using the spICP-MS technique to measure dissolution in complex samples include 1) the measurement of primary particle size as the metric of dissolution is more direct than attempting to measure the increase of Ag^{+} in solution and 2) that this is possible even when known sinks for Ag^{+} exist in the system (*e.g.* DOC, sediments, biota, sampling container).

Received 12th December 2013,
Accepted 18th February 2014

DOI: 10.1039/c3en00108c

rsc.li/es-nano

Nano Impact

Innovative analytical methods are needed to support the detection, characterization, and transformation of nanomaterials in environmental and biological media to assess their potential impacts and support future regulations. Single particle ICP-MS (spICP-MS) is an emergent methodology and its utility is emphasized here in understanding the dynamics of Ag nanoparticle dissolution. Two specific highlights of the benefits of this technique to measure dissolution in complex samples include 1) measuring the primary particle size as the metric of dissolution, which is more direct than attempting to measure increases in Ag^{+} and 2) that this is possible even when known sinks for Ag^{+} exist in the system (*e.g.* sediments, biota, sampling container). The breadth of studies for which spICP-MS may be useful is growing.

[a] *Department of Chemistry and Geochemistry, Colorado School of Mines, Golden, CO, USA*
[b] *Technology and Society Laboratory, Empa – Materials Science and Technology, St. Gallen, Switzerland*
[c] *U.S. Army Engineer Research and Development Center, Vicksburg, MS, USA*
[d] *Department of Applied Mathematics and Statistics, Colorado School of Mines, Golden, CO, USA*
[e] *Department of Civil and Environmental Engineering, Colorado School of Mines, Golden, CO, USA. E-mail: chiggins@mines.edu*

† Electronic supplementary information (ESI) available: Water chemistry, discussion of data collection, processing, and example calculations of dissolution rate kinetics and total system Ag. Results of light and concentration studies. Comparison of variable DOC concentrations. Raw particle size *versus* time data and statistical analysis of rates. See DOI: 10.1039/c3en00108c

Introduction

The unique characteristics of nanomaterials bring a new complexity to the testing of environmental effects. In recent years, progress has been made in understanding the factors influencing engineered nanoparticles' (ENPs) environmental fate and transport including: qualitative risk assessment,[2,3] quantitative exposure modeling,[4,5] industrial production,[6,7] release from products,[8–12] and environmental behavior and effects.[13,14] Recent reviews have tackled pressing concerns including standardizing test methods,[15,16] potential release

scenarios,[17] and transformations in the aquatic environment and in biota.[2,18,19] Producing, using, and disposing of nanomaterials and nano-enabled products will likely lead to their environmental release.[20–22] Much of the fundamental research is being conducted at ENP concentrations above expected environmental concentrations (μg L^{-1} or mg L^{-1} *vs.* ng L^{-1}), which is due in part to the limited number of applicable detection and characterization methods. This approach may alter the understanding of the extent and type of interactions of ENPs and environmental constituents. New techniques, such as single particle ICP-MS (spICP-MS), which allow for the detection and characterization of trace levels of ENPs (*i.e.*, ng L^{-1}) in complex samples, may help alleviate this problem and further illuminate interactions at dilute concentrations.

Understanding the diverse impacts of ENP physical-chemical properties and the large suite of potential geogenic,[23] biogenic,[24] and anthropogenic influences[19] on ENP behavior in the environment is a complex task. ENP environmental transformations are likely to be dependent on a few key environmental and ENP features. Important water chemistry parameters are electrolyte composition and ionic strength, redox environment, pH, and dissolved organic carbon (DOC). Thermodynamic calculations and some kinetic measurements suggest that Ag ENPs will not persist in realistic environmental compartments containing dissolved O_2.[1,18,23,25,26] DOC may slow dissolution through surface adsorption and the subsequent blocking of Ag ENP oxidation sites[27] or through reversible reactions of released Ag^+ returning to Ag^0, with DOC acting as a reductant.[28] DOC may also serve as a competitive sink for oxidants.[29] (Oxy)sulfidation could lead to rapid transformation, particularly when conditions are favorable for the formation of insoluble silver sulfides.[30,31] Other common ligands in natural systems, including Cl^-,[23,32] are known to either complex directly with Ag ENPs or with the Ag^+ released during ENP oxidation.[30,31] With respect to ENP properties, surface modifiers, which are generally designed to impart stability with respect to aggregation, can also provide resistance to dissolution.[25,33] These engineered surface functionalities may be subject to alteration, replacement, or over-coating in the environment, thus reducing their influence. In addition, the preferential dissolution of smaller particle sizes has been suggested.[34] Conversely, others describe the mass-normalized rate of dissolution as nearly independent of particle size.[35] How natural water chemistry will affect particles' transformations and subsequent toxicity is also a matter of open debate, but some preliminary models are now being compiled which attempt to parameterize particle properties and predict nanotoxicity.[36]

Using dynamic light scattering (DLS), asymmetrical flow field flow fractionation (AF4; in some cases coupled to ICP-MS), or imaging techniques such as transmission electron microscopy (TEM), several studies have examined the interactions of solution chemistry with ENPs,[25,33,37] primarily working in the μg to mg L^{-1} range.[24,34] It is not immediately evident whether the same processes affecting ENP behavior at these artificially high concentrations (*i.e.* higher than the predicted environmental concentrations) are the same at lower, environmentally relevant concentrations.[38] Therefore, it is prudent to conduct experiments under more realistic conditions. This study aimed to examine the dissolution of Ag ENPs at environmentally relevant concentrations and to quantitatively evaluate the resultant dissolution rates in a variety of aquatic matrices. Because the dissolution rate is surface area controlled, the time to complete dissolution is highly dependent on the initial and (potentially stable) intermediate particle sizes. By measuring the change in particle size as well as the evolution of $Ag^+_{(aq)}$ in solution, using a technique such as spICP-MS, one may potentially avoid pitfalls related to the loss of Ag^+ to experimental materials and to other environmental surfaces such as suspended sediments or biota in the case of complex systems.

In this study, Ag ENPs of two sizes (60 and 100 nm) and with three capping agents (citrate, tannic acid, and polyvinylpyrrolidone) were suspended in various laboratory, natural, and processed waters to test the spICP-MS protocol for realistic systems and to also discern the factors influencing particle dissolution. Laboratory waters (*i.e.* deionized (DI) water, with the addition of Cl^-, S^{2-}, or DOC) were used to study the influence of anion composition and concentration (stoichiometric and 1 mg L^{-1}) on dissolution as well as the potential stabilizing effects of DOC (2 and 20 mg L^{-1}). U.S. Environmental Protection Agency (EPA) moderately hard reconstituted laboratory water, local stream water, and tap water represented laboratory toxicity test environments and natural and processed waters, respectively. Studies were conducted using spICP-MS at ENP concentrations (ng L^{-1} range) predicted to be environmentally relevant. Notably, the spICP-MS method determined the primary Ag ENP size: any build-up of material or surface complexes (*i.e.* with Cl^-, S^{2-}, DOC) were not analysed in this study.

Materials and methods

Materials

Both 60 and 100 nm diameter Ag ENPs (NanoXact, NanoComposix), having three capping agents, including citrate (C), tannic acid (TA), and polyvinylpyrrolidone (PVP) were examined. The accompanying manufacturer-supplied size information indicated the particles to be monodisperse, with TEM analysis showing the particles as 60 ± 5.3 nm and 100 ± 9.4 nm, and corresponding DLS confirming the nominal particle sizes. Additional characterization was performed by AF4-ICP-MS (AF2000 AT, PostNova Analytics, Perkin Elmer NEXION 300Q, see ESI†), which found particle sizes of 60 ± 5 nm and 100 ± 9 nm, respectively, and differential centrifugal sedimentation analysis (DC 24000, CPS Instruments).[39] In the 100 nm particle suspension, an impurity of a secondary particle at 110 ± 5 nm (<5%) was detected by the centrifugal analysis. Though the 100 nm particles were reported to have an 8 nm Au core, and this was confirmed by AF4-ICP-MS, this core represents <1% of the particle volume, suggesting it has negligible impact on the dissolution processes examined here. No Au core was detected for the 60 nm Ag ENP. The

slightly smaller spICP-MS based size (~90 nm) of the 100 nm particles was possibly due to some degree of porosity (*e.g.* reduced density), which is consistent with the observations of Kaegi *et al.*[40] who observed a polycrystalline nature of 100 nm Nanocomposix ENPs. ENP suspensions were made by diluting stock solutions (20 mg L^{-1} Ag) with an appropriate water composition to a final concentration of 50 ng L^{-1} Ag. To match the peak intensities observed by spICP-MS, dissolved Ag standards (High-Purity Standards; QC-7-M), used for calibration, were diluted in 2% HNO_3 (Optima grade) to concentrations ranging from 0.1–1 μg L^{-1}. The need to calibrate with dissolved standards at concentrations higher than that for the NPs is a consequence of the nebulization efficiency, which delivers only about 2–5% of the Ag mass in the dissolved standards. For determination of the nebulization efficiency (calculated through the particle size approach described in previous literature), 100 nm Au NPs were obtained from BBI and prepared daily as a 100 ng L^{-1} solution in DI water.

Water compositions included DI water (DI, 18.3 M ohm cm Nanopure), tap water (CSM campus), surface water, and EPA moderately hard reconstituted laboratory water. The surface water (Crk) sample, collected in June 2012 from Clear Creek in Golden, CO, was taken just beneath the water surface, approximately 1 m from the stream bank, and passed through a 0.45 micron filter. The sample was stored in a polyethylene bottle at 20 °C prior to use.

Concentrations of common dissolved elements were measured by Inductively Coupled Plasma Optical Emission Spectroscopy (ICP-OES) (Perkin Elmer 5300). Anion concentrations were determined by ion chromatography (Dionex ICS-90). Total organic carbon was measured with a Sievers model 5310C Total Organic Carbon (TOC) analyzer. Tap water samples contained 1.13 ± 0.04 mg L^{-1} residual free chlorine recorded at the Golden, CO water treatment facility. Additional information on water chemistry is provided in Table S1.†

For ENP stability studies, NaCl was added to DI water at 1 mg L^{-1} and equimolar chloride (50 ng L^{-1} Ag ENP; 27.2 ng L^{-1} NaCl). Sulfidation experiments were conducted in an anaerobic chamber for 24 h. Na_2S was added at 1 mg L^{-1} and stoichiometric concentrations (50 ng L^{-1} Ag ENP; 18.2 ng L^{-1} Na_2S), prepared inside the chamber, with DI water sparged with N_2. Suwanee River dissolved organic matter (90% fulvic acid, IHSS) was added to DI water at 2 and 20 mg C L^{-1}.

Methods

Instrumentation. A Perkin Elmer NexION 300Q was used for spICP-MS analysis. The operating conditions were optimized to produce maximum ^{107}Ag intensity. Integration dwell times of 10 ms, and a data collection time of 120 s were used. Instrument calibration utilized a blank and four dissolved Ag solutions (0–1 μg L^{-1}), with data collected in spICP-MS mode. Standards were made both in 2% HNO_3 and in matrices matched to the water chemistry. Acidified samples served as a check standard and a measure of the sensitivity of the instrument, where the latter calibration curve was used for particle sizing. To monitor instrumental drift over time, a single 100 ng L^{-1} Ag dissolved calibration check standard was analysed in spICP-MS mode after every ten ENP samples. If drift in the standard signal was detected, the particle sizing equation was adjusted accordingly for the decrease in sensitivity. If check standard intensities drifted more than 30% in a day, the experiments were repeated, as reproducibility was poor under these conditions. Size analysis for DI water experiments at μg L^{-1} Ag ENP concentrations were also performed by AF4-ICP-MS.

Data collection, conversion to particle size, and quality assurance. For spICP-MS, raw intensity data were plotted as pulse intensity *versus* number of pulses, where any values below the first minimum (moving from low to high intensity) in the histogram were considered background/dissolved (see Fig. S1†). The theoretical basis of spICP-MS detection has been well studied in recent years.[41–46] In this study, background/dissolved counts were subtracted from the pulse intensity, and ENPs were sized[41,46] using a density of 10.5 gm cm^{-3}, the nebulization efficiency determined by analysis of the Au ENPs, and assuming complete ionization of the particles in the plasma. Previous studies indicated that nanometer-sized Ag particles are completely ablated in the plasma.[43,47,48] Determination of the transport efficiency is critical to computing ENP size when using an approach based on calibration with dissolved standards. We therefore measured this parameter at the start of each day's analysis and checked its value several times during the analysis. To avoid particle coincidence, concentrations were used whereby <15% of the measurements were ENP pulses.[41,45]

Characterization of particle dissolution and silver release. The dissolution of particles was studied over seven days. All samples in a dissolution set were analyzed in a single day by staggering the start of dissolution for each time point. Each set consisted of a given water chemistry and particle size, including all particle coatings and time points, performed in triplicate. Time points included 0, 1, 2, 4, 8, 12, 24, 96, and 168 h, with some sets excluding the last two time points. For all sample sets, T = 0 h represents immediate sample analysis after ENP spiking. All samples were shaken by hand prior to analysis. Once differentiation between dissolved and ENP fractions was made, each fraction was quantified. For the dissolved fraction, this was *via* direct comparison to the dissolved calibration curve. For the ENP fraction, once the mean dissolved background intensity was subtracted from the pulse intensity, counts were converted to mass, which subsequently enabled calculations of both ENP diameter and, using measured transport efficiency, mass/number concentrations.[41] Further details can be found in the ESI.† The minimum detectable ENP size was typically 25–30 nm. Contributing factors that tended to increase the minimum size detection limit included decreased ICP-MS sensitivity, matrix signal suppression, salting of the cones, and increased background $Ag_{(aq)}$. While the differentiation of the background and ENP signals was almost always possible, in some

cases, quantification of Ag^+ accumulation over time was not possible. This was especially evident in complex matrices, where Ag^+ was either obscured by the background signal due to decreased instrumental sensitivity, complexed to matrix constituents (*e.g.* DOC), or was lost to experimental materials (*e.g.* sample tubes).

Total Ag components (NP and ionic) were tracked for all dissolution sets to include: 1) dissolved Ag^+ concentration from the background signal; and 2) particle mass concentration as calculated by summation of the particle mass analysed (corrected for particle transport efficiency). For each time point <24 h, these two concentrations were summed to provide the total Ag directly measured as dissolved and ENP mass concentrations. As particle number concentrations changed over time and likely contributed to deviations from complete mass balance, mass balance calculations were repeated for these data sets using the measured dissolved Ag^+ concentration but adjusting the ENP mass for the fraction of particles not directly measured. This second approach assumes that the size distributions of any ENPs not directly measured (due to sticking to the sample tube, *etc.*) are identical to the ENPs remaining in solution.

Dissolution rate kinetics. Using the instantaneous average particle diameter, the mass of Ag lost from the original particle was calculated. After normalizing by calculated geometric surface area for that size particle (assuming spherical particles), the mass of Ag lost per surface area (mol cm^{-2}) *versus* time was examined to obtain the dissolution rate constant. As ENP dissolution has been shown to follow first-order kinetics under relatively short time periods (under 48 h) at low (<1 μg L^{-1}) total Ag concentrations,[49] first-order dissolution kinetics were initially assumed. However, an inspection of the resultant data indicated that the dissolution rate was not necessarily constant for all time points, two rates were calculated for longer (up to 168 h) experiments: one rate for <24 h and one for time points >24 h. Rate constants were calculated for all systems where the particles showed a 10% change in diameter or more over the experimental time period and average rate constants were calculated as the average of the log-transformed rate constants for individual experiments. Additional details can be found in the ESI.†

Statistical analysis. Comparisons of the <24 h log dissolution rates were conducted across various combinations of particle size, capping agent, and water type using the statistical software package R. A full factorial model could not be used since dissolution rates were not measurable in all cases (*e.g.* 60 nm particles with DOC). Instead, an initial three-way ANOVA was conducted with size (60 nm and 100 nm), capping agent (C, TA, and PVP), and water composition (DI, Crk, and Tap) as factors. In this analysis, all pair-wise and three-way interactions were significant, so we were unable to draw conclusions about the main effects of each factor. Consequently, pair-wise comparisons of the log dissolution rates were conducted across unique pairs of testing conditions using Tukey's Honestly Significant Difference (HSD) test.[50] When conducting pair-wise comparisons, rates for 100 nm particles in DOC water were also included in the analysis. Table S3† provides the *p*-values obtained after adjustments for multiple comparisons, with values less than or equal to 0.05 indicating significance at a 95% family-wise confidence level.

Additionally, <24 h and >24 h log dissolution rates were compared across all testing combinations of size, capping agent, and water composition that were measured for both time intervals. This analysis was conducted using log differences, defined as $\log(r > 24\text{ h}, ij) - \log(r < 24\text{ h}, ij) = \log(r > 24\text{ h}, ij/r < 24\text{ h}, ij)$, where $r < 24$ h, ij and $r > 24$ h, ij denote the dissolution rates measured for the j^{th} replicate of treatment i across the <24 h and >24 h time intervals, respectively. An initial linear regression that included all main factors and their interaction terms was fit to the log differences in order to assess whether changes in rates over time varied significantly across different treatments. Finding no significant evidence that particle size, capping agent, water type, or their interactions explained any of the variability in the log differences, a *t*-test was conducted to assess the overall change in rates from the <24 h interval to the >24 h interval.

Preliminary control studies. All dissolution experiments were conducted at ambient temperature (approximately 23 °C). A recent study observed UV-enhanced dissolution (*i.e.*, photo oxidation) under intense UV lights. To ensure minimal photo-enhanced dissolution under ambient laboratory lighting, dissolution was initially examined with 100 nm citrate capped Ag ENPs in DI water for 12 h with various light treatments including: natural (window) light, ambient laboratory light, and in the dark. As detailed in Table S2,† minimal lighting effects were observed (in agreement with other published studies[1,26]), and as a result, all further experiments were conducted under ambient laboratory light. The importance of working at environmentally relevant concentrations (*i.e.*, ng Ag L^{-1}) was also tested by performing a limited set of preliminary experiments with a suspension of 50 μg L^{-1} 60 nm TA Ag ENPs in DI. At one hour time intervals (up to 12 h), samples were analysed by (1) direct injection of the sample into the AF4-ICP-MS and (2) dilution to 50 ng L^{-1} in DI, with immediate analysis by spICP-MS.

Results and discussion

Preliminary control studies and total silver mass balances

No detectable dissolution of 60 nm TA Ag ENPs at 50 μg L^{-1} (Fig. S2†) over 12 h was found by both AF4-ICP-MS and spICP-MS, in direct contrast to our dissolution kinetics results observed at lower concentrations. For example, data demonstrating the dissolution of 100 nm TA Ag ENPs (50 ng L^{-1}) in DI are provided in Fig. 1, with the decrease in raw pulse intensities being direct evidence of size reduction over time. The corresponding Ag^+ increase over time was observed in most experiments. While the Ag mass balance decreased over time in almost all 100 nm experiments, the overall mass balance (measured ENP plus dissolved Ag^+), was generally

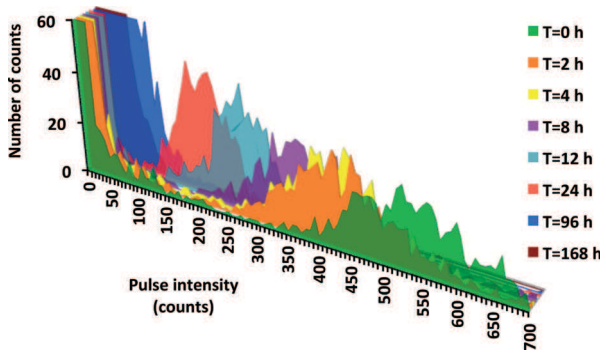

Fig. 1 Dissolution of 100 nm TA capped Ag ENPs at 50 ng L^{-1} over time, as evidenced by the decrease in pulse intensity over time. Raw pulse intensity is proportional to particle mass (*x*-axis) and so smaller pulses indicate less Ag associated with each particle. The number of particles observed (*y*-axis) is similar for each analysis.

fairly good, with the overall average mass balance (unadjusted for loss of ENPs) for all 100 nm particles in all water types of 88 ± 15% (Table S4†). After adjusting for the few cases where ENP number decreased over time, the overall mass balance increased to 94 ± 15%. From a mass balance perspective, the most problematic experiments were those employing filtered Creek water. Fig. S3† exemplifies this trend, with DI and Creek water, showing measured Ag^+ and ENP concentrations, with total Ag being a summation of these two fractions. In the later samples, there was a deficit in the total Ag concentration over time. Two factors may be responsible for this: 1) a decrease in ENP number analysed over time and/or 2) an inability to detect Ag^+, possibly due to loss of Ag^+ to the container. In Creek water, this difference is more dramatic. In any investigation of environmental samples, if particle number concentration is desired, sample holding times must be short and/or alternative sample containers might need to be investigated to improve particle recovery. Nevertheless, the overall good agreement with respect to the mass balances achieved strongly supports the validity of using spICP-MS for quantitative evaluations of ENP dissolution rates.

Dissolution rates in DI water

As is evident in Fig. 2, the calculated surface area-normalized mass loss of $Ag^+_{(aq)}$ from the 100 nm particles in DI water is roughly linear in time, consistent with steady-state dissolution, until 24 h, whereupon the dissolution rate slows (Fig. 2A). Similarly, as shown in Fig. 2B, the instantaneous Ag dissolution rates are generally steady for the first 24 h. An exception to this is the TA-coated particles, where a slightly higher (but slowing) dissolution rate is suggested during the first few hours in DI water. As the development of the mechanistic underpinnings for non first-order rates of dissolution was beyond the scope of the present study, first-order dissolution rates were calculated from the data, though different rates were calculated from the first 24 h as compared to >24 h. While somewhat arbitrary, this 24 h breakpoint was observed in nearly all data sets. The statistical evaluation of this breakpoint determined that the estimated average log difference was −0.64 (p-value < 0.001) with corresponding 95% confidence interval (−0.81, −0.47), indicating a significant overall decrease in log dissolution rates after the initial 24 h. A summary of the results for the experiments in which dissolution was measurable is provided in Table 1 with separate rates of dissolution for time points before and after 24 h. Variance in the calculated dissolution rates for experiments <24 h can be seen in Fig. 3. Time points longer than 24 hours were not included because data were not collected in this time period for all experimental sets.

The statistical analysis of <24 h and >24 h log dissolution rates indicates that there is significant evidence of a decrease in log dissolution rates during the >24 h time interval. The complex dissolution kinetics observed were somewhat unexpected. While an initial release of sorbed Ag^+ from the ENP surface has been suggested for Ag ENPs fixed in gel

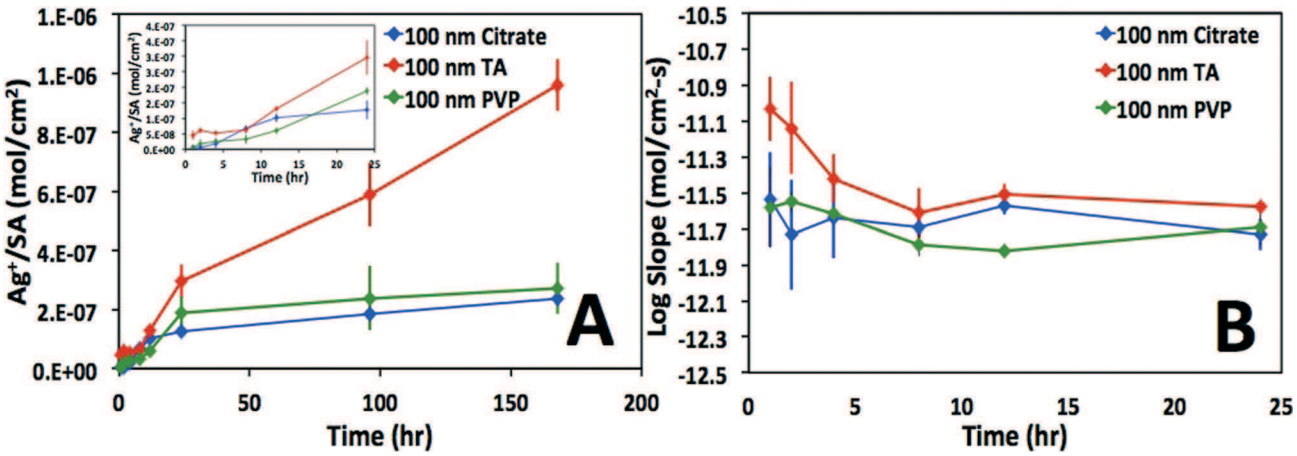

Fig. 2 Temporal variation in dissolution rates and instantaneous dissolution rates for a representative dissolution experiment of 50 ng L^{-1} Ag ENP (DI water). Blue, red, and green traces represent citrate, TA, and PVP coatings, respectively. Panel A: geometric surface area normalized to the calculated mass of Ag released from particles over time (inset, 24 h time period) and Panel B: instantaneous dissolution rates. Error bars represent the standard deviation from triplicate experiments.

Table 1 Summary of average dissolution rates. Abbreviations: Clear Creek water (Crk) and 2 mg L^{-1} DOC (DOC). Literature calculated values are estimated based on the equation developed by Liu and Hurt[1] and pH, DOC, and temperature values are provided in Table S1, assuming NOM = 2 × DOC

Water chemistry	Surface coating	100 nm $t < 24$ h log r/(mol cm^{-2} s^{-1})	100 nm $t > 24$ h log r/(mol cm^{-2} s^{-1})	60 nm $t < 24$ h log r/(mol cm^{-2} s^{-1})	60 nm $t > 24$ h log r/(mol cm^{-2} s^{-1})	Literature calculated log r/(mol cm^{-2} s^{-1})
DI	C	−11.72 ± 0.07	−12.59 ± 0.15	−12.23 ± 0.09	−13.12 ± 0.29	−13.62
DI	TA	−11.62 ± 0.11	−11.92 ± 0.02	−11.80 ± 0.04		
DI	PVP	−11.78 ± 0.13	−12.71 ± 0.07	−12.62 ± 0.07	−12.57 ± 0.26	
Tap	C	−11.32 ± 0.05		−11.64 ± 0.13		−13.90
Tap	TA	−11.18 ± 0.006		−11.76 ± 0.11		
Tap	PVP	−11.56 ± 0.21		−11.88 ± 0.09		
Crk	C	−12.14 ± 0.09	−13.07 ± 1.03	−12.71 ± 0.14	−13.14 ± 0.16	−13.90
Crk	TA	−12.49 ± 0.10	−13.34 ± 0.56	−12.38 ± 0.10	−12.88 ± 0.12	
Crk	PVP	−12.33 ± 0.03	−12.03 ± 0.18	−12.36 ± 0.12	−13.03 ± 0.16	
DOC	C	−12.46 ± 0.09				−13.42
DOC	TA	−12.57 ± 0.13				
DOC	PVP	−12.16 ± 0.07				

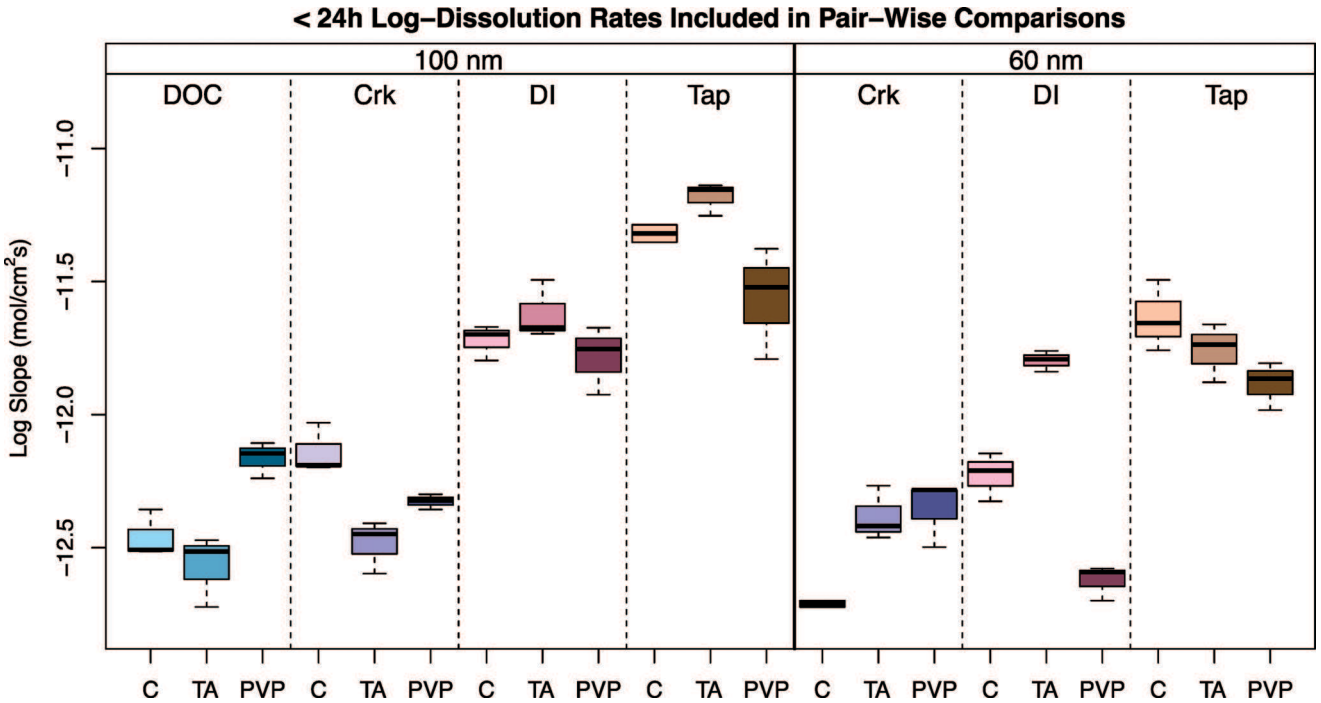

Fig. 3 Boxplots of the <24 h log dissolution rates for treatments included in the pair-wise comparisons of Table S3.†

pucks and suspended in natural waters,[51] it is unlikely that the change in size associated with the faster initial rates in the present study (up to ~70% loss of Ag ENP mass) was attributable to this process. While it is possible that after substantial surface oxidation and partial dissolution, a shell of oxidized Ag (similar to that observed by Gorham *et al.*[52]) inhibits further dissolution, it is not immediately evident if this is the appropriate mechanistic explanation for the data described herein. Clearly, further research is needed to fully elucidate the mechanisms resulting in these complex dissolution kinetics.

Effects of water chemistry on ENP stability

A comparison of the results in simple laboratory-prepared waters, including DI water and additions of chloride, sulfide, or DOC, is found in Fig. 4. Dissolution of 60 and 100 nm ENPs in DI water (Fig. 4A) results in the largest decrease in diameter within the first 24 h. The dissolution rates for experimental sets with more than 10% diameter decrease over 24 h can be found in Table 1; additional details as to how these rates were calculated and statistical comparisons are provided in the ESI.† A slower but steady subsequent decline in rate over the remaining 144 h is observed, with a rate up to an order of magnitude lower ($10^{-12.6}$ mol cm^{-2} s^{-1}) for 100 nm particles in the second time block (24–168 h). Without additional time points, it is difficult to ascertain if the second phase is steady state dissolution. Rates varied slightly with particle surface coating, ranging up to a difference of 0.5 log units between coatings under the same conditions. In most instances, TA capped particles showed faster

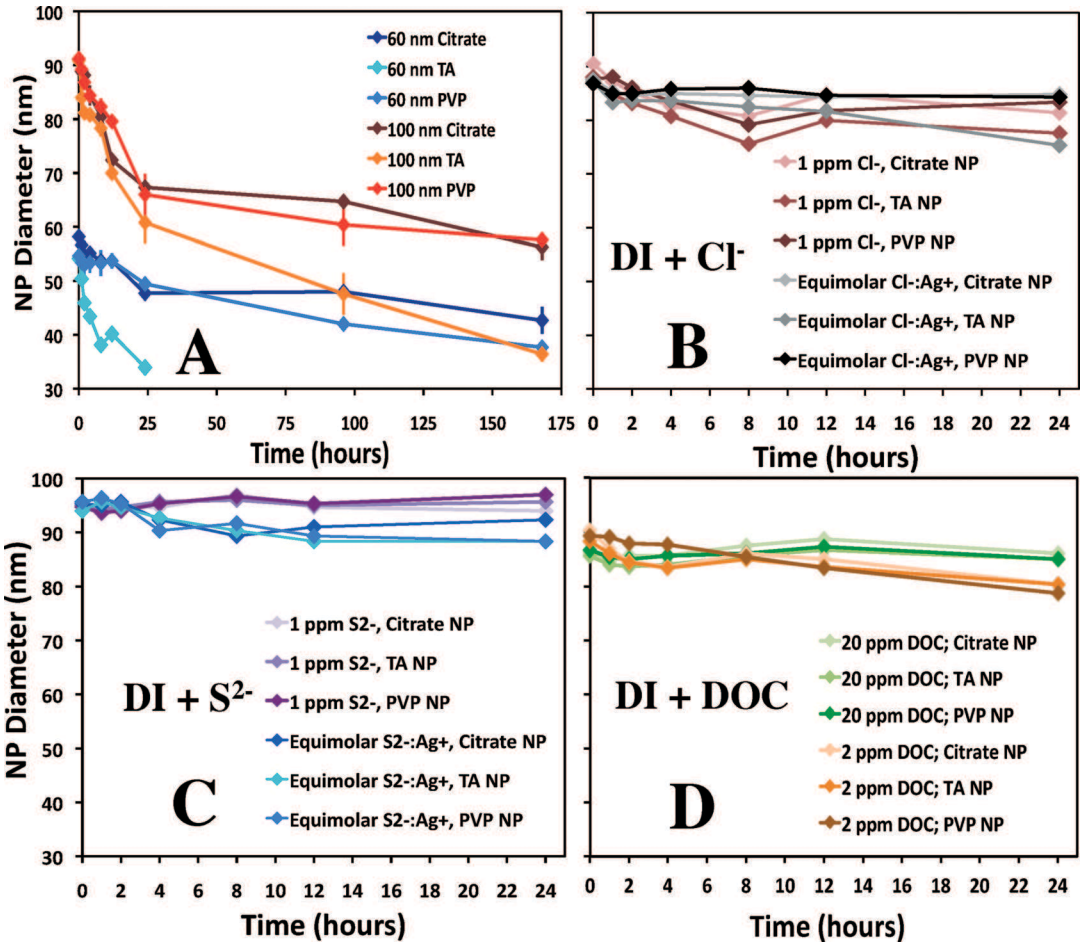

Fig. 4 Summary of Ag ENP dissolution, at 50 ng L^{-1}, in simple systems. Panel A: comparison of 60 nm and 100 nm ENPs in DI water. Panel B: addition of 1 mg L^{-1} and equimolar Cl^-. Panel C: addition of 1 mg L^{-1} and equimolar S^{2-}. Panel D: Addition of 20 and 2 mg L^{-1} DOC. Note that the approximate detection limit of 30 nm was reached for the 60 nm TA sample. Error bars represent the standard deviation of triplicate experiments.

dissolution (up to 0.9 log units) compared to either the citrate or PVP coatings. In the first 24 h, the 100 nm TA capped ENP diameters had decreased up to 15% more, while after 168 h, the diameter was nearly 40% smaller than the PVP ENPs.

To enable comparisons of the observed rates of dissolution to literature values, an equation developed by Liu and Hurt[1] was used to estimate dissolution rates for a subset of conditions (Table 1), fully recognizing that this equation did not account for all factors that likely influenced the rate of dissolution (*i.e.*, oxidants, ENP coating, *etc.*). Liu and Hurt examined the dissolution of 2 nm citrate Ag ENPs,[1] measuring Ag^+ accumulation in solution until a seemingly steady state was achieved (between 6 and 125 d). When the empirical equation derived by Liu and Hurt was used to estimate the rates of dissolution in the present study, the rates were, in general, significantly slower (up to ~100×) than the rates observed herein, but relatively close, given the significant differences in experimental approach (concentration and size of ENPs, analysis type, *etc.*). In some cases (*i.e.* tap water), large differences would be expected, as the empirical equation did not account for factors such as the presence of a chlorine residual. However, the fact that the rates were generally faster, when coupled to the complex kinetics observed, suggests that additional investigations into Ag ENP dissolution are warranted.

With the addition of Cl^- (Fig. 4B), little to no change in ENP size was detected, depending on the particle coating and Cl^- concentration. The more concentrated 1 ppm Cl^- hindered dissolution more than the equimolar $Cl^-:Ag^+$ experiment; an approximately 10% difference in diameter after 24 h was observed in the latter experiment. For comparison to this study, using approximately 5 nm Ag ENPs (0.001–0.1 mM), Ho *et al.* determined pseudo-first-order rate constants for Ag ENP dissolution in the presence of H_2O_2.[53] A dramatic decrease in dissolution rate was observed with one equivalent of Cl^- (0.05 mM), and dissolution was undetectable when 1 mM Cl^- was used. The authors suggest halide binding to the surface slowed down the etching of Ag ENPs by blocking the added H_2O_2, which limited dissolution, a scenario that may have also prevented further oxidation in the present study.

With respect to the effects of sulfide, the trend is clear that there is no dissolution after 24 h (Fig. 4C). Though the formation of a silver sulfide layer on the particle surface may

actually increase particle size (as has been observed[54]), this would not be evident using spICP-MS, as the total mass of Ag (what is measured in spICP-MS) is unlikely to increase. Formation of a relatively insoluble metal–sulfide shell on the particle surface can potentially 1) inhibit further dissolution or 2) alter the surface charge and induce aggregation.[30] Liu *et al.* suggested two mechanisms of sulfidation depending on sulfide concentration.[31] At high sulfide concentrations they propose the direct conversion of Ag-ENPs to Ag_2S NPs, or, at lower concentrations, the oxidative dissolution of Ag ENPs followed by sulfide precipitation. Even small amounts of sulfur (S : Ag ratio of 0.02) reduced Ag ENP solubility 7-fold compared to the control, with no Ag^+ release detected at S : Ag > 0.43.[30] Furthermore, these complexes did not oxidize after a prolonged (18 h) aeration, suggesting that after Ag_2S shell formation, the possibility of further oxidative dissolution is negligible. In comparison to the present study, minimal (*i.e.* unobservable) dissolution was evident at higher (1 mg L^{-1}) S^{2-} concentrations, though slight decreases in diameter were detected at stoichiometric S^{2-} Ag concentrations. This latter observation may be explained by a pre-oxidation step: where Ag^+ forms on the surface and reacts with sulfide homogeneously to form distinct Ag_2S particles.[31,54] Notably, the formation of new particles (*i.e.* AgCl or Ag_2S complexes) greater than ~30 nm was not observed in the present study.

Finally, despite the resultant drop in pH (6.7 to 4.2; Table S1†) upon the addition of Suwanee River DOM to DI water, the addition of 20 mg L^{-1} DOC essentially halted Ag ENP dissolution, though the 2 mg L^{-1} DOC dissolution data set suggested a slight diameter decrease (near 10%) over 24 h (Fig. 4D). The dissolution rate of 100 nm particles with 2 mg L^{-1} DOC averaged $10^{-12.4}$ mol cm^{-2} s^{-1} between the various capping agents, approximately 0.7 log units (~5×) slower than the DI dissolution set. Likewise, in other studies, DOC has been shown to increase particle stability, which is postulated to be due to both providing a physical barrier to oxidation and changing the surface charge.[55] Microscopy studies investigating the complexation of DOC and ENPs showed general aggregate complexes and did not discern the effect of DOC on individual particles,[26,37,56] though this may be because 1) higher concentrations of particles induced aggregation more readily or 2) imaging techniques are not effective in capturing individual ENP transformations. We suspect that if aggregation had occurred, it would be evidenced by increased pulse intensities and reduced pulse number. While reduced pulse number was generally observed in the presence of DOC, the pulse intensities did not increase, suggesting Ag ENP aggregation was not occurring.

Environmental systems

Slight variations in the size of the nominal 100 nm Ag ENPs were detected, regardless of capping agent, over a seven-day period (Fig. 5A) in environmentally relevant waters. As seen in Fig. 5B, for Clear Creek water, slightly more dissolution than in the EPA moderately hard water was observed, where both the 60 and 100 nm samples decreased just over 15% in

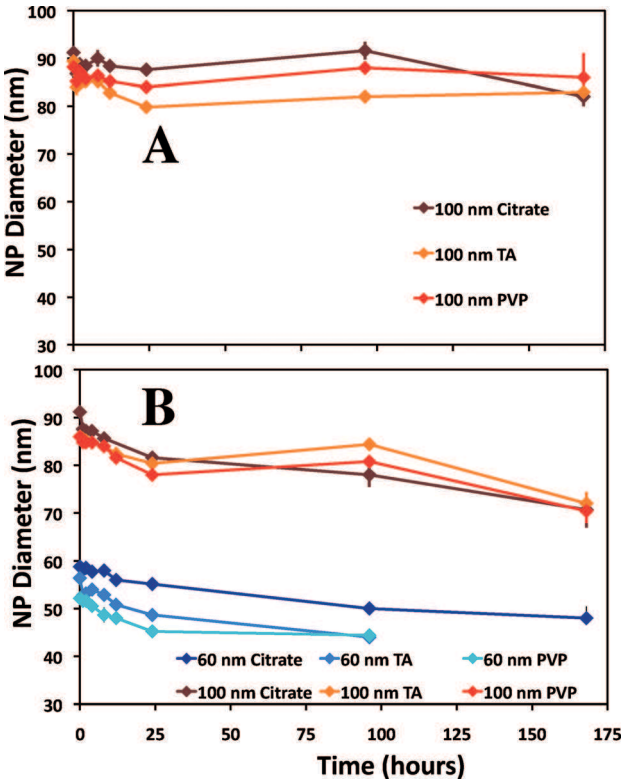

Fig. 5 Summary of Ag NP dissolution, 50 ng L^{-1}, in environmentally relevant water systems. Panel A: EPA moderately hard water. Panel B: Clear Creek water, Golden, CO. Error bars represent the standard deviation of triplicate experiments.

particle diameter over seven days. Natural systems are inherently complex, and thus difficulties arise in making direct comparisons to other published studies. In one example from Li and Lenhart, the aggregation and dissolution of Ag ENPs in river water was examined over 15 d.[26] The authors note substantial aggregation of citrate particles after six hours, in contrast to the present study, though aggregation may have been induced due to the higher particle number concentrations (5.2×10^8 particles mL^{-1} *versus* 8.43×10^4 particles mL^{-1} and 1.82×10^4 particles mL^{-1} for 60 and 100 nm particles, respectively, herein). However, the results from the present study suggest DOC may be one of the most relevant predictors of dissolution in natural waters. For example, in Fig. 6, for both the 2 mg L^{-1} DOC in DI water experiment and the Clear Creek experiment (which contained approximately 2 mg L^{-1} DOC), the dissolution rates are similar over the 24 h time period ($10^{-12.46}$ mol cm^{-2} s^{-1} *vs.* $10^{-12.14}$ mol cm^2 s^{-1}; citrate capped ENPs; Fig. 3) despite significant differences in major ion chemistry. While these correlations can be made in these simple systems, it is unlikely that DOC concentration alone dictates the dissolution rate of Ag ENPs in more complex environmental scenarios.

Dissolution in tap water

Dissolution in chlorine-containing tap water was faster than all other solutions examined (Fig. 7), averaging an increased

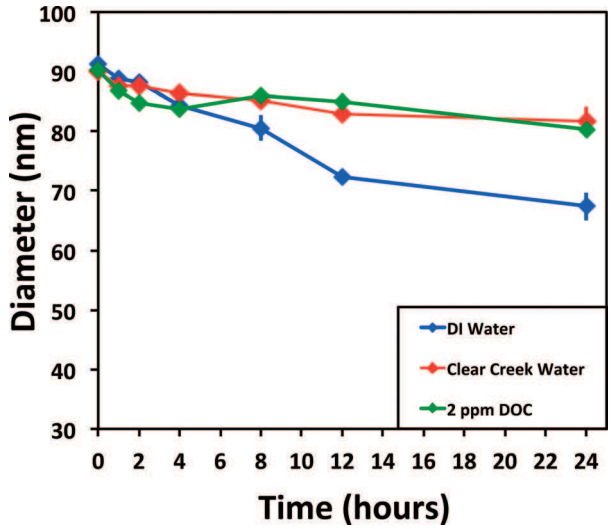

Fig. 6 Creek and DOC spiked water, both with approximately 2 mg L^{-1} DOC, compared to DI water. Apparent similar dissolution rates due to DOC. Error bars represent the standard deviation of triplicate experiments.

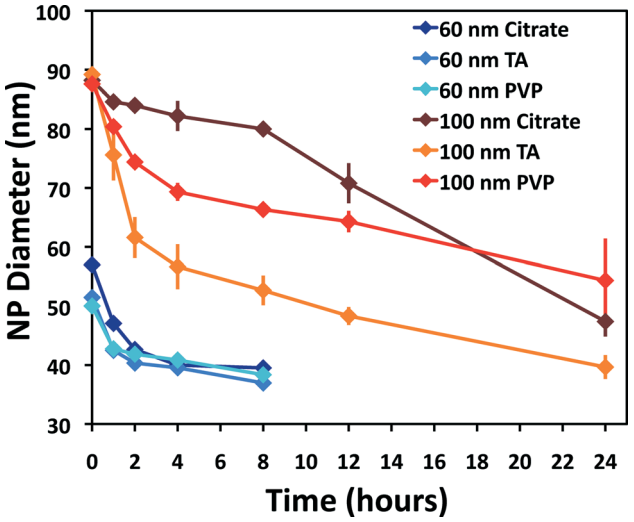

Fig. 7 Summary of Ag ENP dissolution, 50 ng L^{-1} in tap water. Limited time points were collected for 60 nm samples as they decreased below the method detection limit at later time points. Error bars represent the standard deviation of triplicate experiments.

dissolution rate of 0.4–0.9 log units compared to DI and Creek water, respectively, for 100 nm particles. For 60 nm particles, the first eight hours of data were collected, after which particles were below the size detection limit of the method. To the best of our knowledge, there are no studies attempting to directly characterize Ag ENP dissolution in tap water outright. However, studies have been performed to understand the washing behavior of materials embedded with Ag ENPs, in which tap water was used, such as adding a hypochlorite/detergent solution,[57] particle release due to simulated washing,[8] or characterization of effluent from a nanosilver producing washing machine.[12]

Trends in Ag ENP dissolution

There are several general trends that can be garnered from Table 1, Table S3,† and Fig. 3. First, in most cases, Ag ENP size appears to be a controlling factor in the dissolution rate. In contrast to predictions from theory, for a given water type and capping agent the 60 nm particles often dissolved slower than 100 nm particles during the <24 h time interval. While not directly comparable, a study of Ag ENP sulfidation suggested that sulfidation of larger Ag ENPs was somewhat faster, when normalized to ENP surface area, than the sulfidation rates for smaller Ag ENPs.[40] Statistically significant differences in surface-normalized dissolution rates were observed for the different sized particles. For example, for citrate-coated particles in DI water, different (p = <0.001) dissolution rates of approximately $10^{-12.2}$ mol cm^{-2} s^{-1} and $10^{-11.7}$ mol cm^{-2} s^{-1} were calculated for 60 and 100 nm particles, respectively. This indicates smaller particles are releasing less Ag^+ per surface area, which has also been observed in other studies.[51,58] This seeming disparity in the inverse relationship between geometric surface area and particle size, as it should relate to dissolution kinetics, might be explained by the polycrystallinity of the 100 nm Nanocomposix Ag ENPs. An elevated sulfidation rate, which may be analogous to dissolution rate, was seen for these same particles in a study by Kaegi *et al.*[59] This observation was explained as an effect of the additional surface area present at the grain boundaries.

Second, variable dissolution rates were observed for different particle coatings. The TA ENPs were generally the least resistant to dissolution, whereas the PVP ENPs were generally more stable (some exceptions noted, see ESI†). However, the effects of ENP coating may become irrelevant in natural waters, as no statistically different rates among coatings were observed for either the 60 or 100 nm Ag ENPs in Creek water (Table S3†). For most circumstances, increasing dissolution rates were observed from creek to DI to tap waters. Dissolution rates also generally slowed after 24 h compared to the initial rates in any given experiment, suggesting that a single dissolution rate may not be appropriate for predicting Ag ENP dissolution, even under a given set of environmental conditions.

Conclusions

Dissolution potential could be a key component of the screening process for categorizing ENPs with common hazard potential based on their release of ionic species. However, simple correlations between dissolution and the physical-chemical properties of ENPs are often difficult to characterize because of the myriad of particle types, capping agents, and complexity of the systems being studied. Often, a change in one parameter will significantly change the extent of dissolution, and determining how multiple factors may co-vary is exceedingly difficult. Generally, environmental exposures are likely to be at low concentration over long time scales, allowing for slow or multiple transformations of the ENPs.

A number of analytical techniques will likely have to be used in conjunction with extrapolating calculations to understand the multitude of ENP interactions with exposure media.

This study demonstrates the utility of spICP-MS to quantitatively evaluate dissolution kinetics for Ag ENPs under a wide range of conditions. This is particularly important in that only a limited number of methods can be directly applied to aqueous samples, especially considering expected ENP concentrations.[60] The available techniques currently used are generally not capable of measuring transformation *in situ* (or *in vivo*) at these concentrations. In addition to filling this gap in metrology, this study demonstrates that spICP-MS can track the rate and extent of transformations of nanomaterials under realistic conditions. Two specific highlights of the benefits of using the spICP-MS technique to measure dissolution in complex samples include 1) the measurement of primary particle size as the metric of dissolution is more direct than attempting to measure the increase of Ag^+ in solution and 2) that this is possible even when known sinks for Ag^+ exist in the system (*e.g.* sediments, biota, sampling container). In laboratory experiments, where particle concentration/number is known, tracking changes in this metric over time can also be valuable. Finally, used as a high-throughput quantitative screening tool, this method could elucidate trends in ENP behavior accurately and quickly.

Acknowledgements

The authors thank the U.S. Army Corps of Engineers (W912HZ-09-P-0163) for funding. Dr. Bernd Nowack and three anonymous reviewers provided valuable comments during manuscript review.

Notes and references

1 J. Liu and R. Hurt, Ion release kinetics and particle persistence in aqueous nano-silver colloids, *Environ. Sci. Technol.*, 2010, **44**(6), 2169–2175.

2 F. von der Kammer, P. L. Ferguson, P. A. Holden, A. Masion, K. R. Rogers, S. J. Klaine, A. A. Koelmans, N. Horne and J. M. Unrine, Analysis of engineered nanomterials in complex matrices (environment and biota): General considerations and conceptual case studies, *Environ. Toxicol. Chem.*, 2012, **31**(1), 32–49.

3 M. Hassellov, J. Readman, J. Ranville and K. Tiede, Nanoparticle analysis and characterization methodologies in environmental risk assessment of engineered nanoparticles, *Ecotoxicology*, 2008, **17**(5), 344–361.

4 A. Praetorius, M. Scheringer and K. Hungerbuhler, Development of Environmental Fate Models for Engineered Nanoparticles—A Case Study of TiO2 Nanoparticles in the Rhine River, *Environ. Sci. Technol.*, 2012, **46**(12), 6705–6713.

5 F. Gottschalk, R. Scholz and B. Nowack, Probabilistic material flow modeling for assessing the environmental exposure to compounds: Methodology and an application to engineered nano-TiO2 particles, *Environmental Modeling & Software*, 2010, **25**(3), 320–332.

6 F. Piccinno, F. Gottschalk, S. Seeger and B. Nowack, Industrial production quantities and uses of ten engineered nanomaterials in Europe and the world, *J. Nanopart. Res.*, 2012, **14**(9), 1–11.

7 C. O. Hendren, X. Mesnard, J. Droage and M. R. Wiesner, Estimating production data for five engineered nanomaterials as a basis for exposure assessment, *Environ. Sci. Technol.*, 2011, **45**(7), 2562–2569.

8 T. M. Benn, B. Cavanagh, K. Hristovski, J. D. Posner and P. Westerhoff, The release of nanosilver from consumer products used in the home, *J. Environ. Qual.*, 2010, **39**, 1875–1882.

9 R. Kaegi, B. Sinnet, S. Zuleeg, H. Hagendorfer, H. Simmler, S. Brunner, H. Vonmont, M. Burkhardt and M. Boller, Synthetic TiO2 nanoparticle emission from exterior facades into the aquatic environment, *Environ. Pollut.*, 2008, **156**, 233–239.

10 R. Kaegi, B. Sinnet, S. Zuleeg, H. Hagendorfer, N. C. Mueller, R. Vonbank, M. Boller and M. Burkhardt, Release of silver nanoparticles from outdoor facades, *Environ. Pollut.*, 2010, **158**, 2900–2905.

11 M. Vorbau, L. Hillemann and M. Stintz, Method for the characterization of the abrasion induced nanoparticle relase into the air from surface coatings, *J. Aerosol Sci.*, 2009, **40**, 209–217.

12 J. Farkas, H. Peter, P. Christian, J. A. Gallego Urrea, M. Hasselloev, J. Tuoriniemi, S. Gustafsson, E. Olsson, K. Hylland and K. V. Thomas, Characterization of the effluent from a nanosilver producing washing machine, *Environ. Int.*, 2011, **36**(6), 1057–1062.

13 J. T. K. Quik, J. A. Vonk, S. F. Hansen, A. Baun and D. Van De Meent, How to assess exposure of aquatic organisms to manufactured nanoparticles?, *Environ. Int.*, 2011, **37**(6), 1068–1077.

14 P. Westerhoff and B. Nowack, Searching for Global Descriptors of Engineered Nanomaterial Fate and Transport in the Environment, *Acc. Chem. Res.*, 2013, **46**(3), 844–853.

15 R. Handy, G. Cornelis, T. Fernandes, O. Tsyusko, A. Decho, S. Sabo-Attwood, C. Metcalfe, J. Steevens, S. J. Klaine, A. A. Koelmans and N. Horne, Ecotoxicity test methods for engineered nanomaterials: Practical experiences and recommendations from the bench, *Environ. Toxicol. Chem.*, 2012, **31**(1), 15–31.

16 I. Romer, T. A. White, M. Baalousha, K. Chipman, M. R. Viant and J. R. Lead, Aggregation and dispersion of silver nanoparticles in exposure media for aquatic toxicity tests, *J. Chromatogr. A*, 2011, **1218**(27), 4226–4233.

17 B. Nowack, J. F. Ranville, S. Diamond, J. A. Gallego-Urrea, C. Metcalfe, J. Rose, N. Horne, A. A. Koelmans and S. J. Klaine, Potential scenarios for nanomaterial release and subsequent alteration in the environment, *Environ. Toxicol. Chem.*, 2012, **31**(1), 50–59.

18 J. Fabrega, S. N. Luoma, C. R. Tyler, T. S. Galloway and J. R. Lead, Silver nanoparticles: Behaviour and effects in the aquatic environment, *Environ. Int.*, 2011, **37**(2), 517–531.

19 G. V. Lowry, K. B. Gregory, S. C. Apte and J. R. Lead, Transformations of Nanomaterials in the Environment, *Environ. Sci. Technol.*, 2012, **46**(13), 6893–6899.
20 F. Gottschalk, T. Sonderer, R. Scholz and B. Nowack, Modeled environmental concentrations of engineered nanomaterials (TiO2, ZnO, Ag, CNT, fullerenes) for different regions, *Environ. Sci. Technol.*, 2009, **43**(24), 9216–9222.
21 B. Nowack, Is anything out there? What life cycle perspectives of nano-products can tell us about nano-particles in the environment, *Nano Today*, 2009, **4**(1), 11–12.
22 N. Mueller and B. Nowack, Exposure modeling of engineered nanoparticles in the environment, *Environ. Sci. Technol.*, 2008, **42**(12), 4447–4453.
23 C. Levard, E. M. Hotze, G. V. Lowry and G. E. Brown Jr, Environmental Transformations of Silver Nanoparticles: Impact on Stability and Toxicity, *Environ. Sci. Technol.*, 2012, **46**(13), 6900–6914.
24 J. M. Unrine, B. P. Colman, A. J. Bone, A. P. Gondikas and C. W. Matson, Biotic and Abiotic Interactions in Aquatic Microcosms Determine Fate and Toxicity of Ag Nanoparticles. Part 1. Aggregation and Dissolution, *Environ. Sci. Technol.*, 2012, **46**(13), 6915.
25 X. Li, J. Lenhart and H. W. Walker, Aggregation Kinetics and Dissolution of Coated Silver Nanoparticles, *Langmuir*, 2012, **28**(2), 1095–1104.
26 X. Li and J. J. Lenhart, Aggregation and Dissolution of Silver Nanoparticles in Natural Surface Water, *Environ. Sci. Technol.*, 2012, **46**(10), 5378–5386.
27 S. Dubas and V. Pimpan, Humic acid assisted synthesis of silver nanoparticles and its application to herbicide detection, *Mater. Lett.*, 2008, **68**, 2661–2663.
28 D. S. Sal'nikov, A. S. Pogorelova, S. V. Makarov and I. Y. Vashurina, Silver ion reduction with peat fulvic acids, *Russ. J. Appl. Chem.*, 2009, **82**(4), 545–548.
29 G. S. Wan, C. H. Liao and F. J. Wu, Photodegradation of humic acid in the presence of hydrogen peroxide, *Chemosphere*, 2001, **42**(4), 379–387.
30 C. Levard, B. C. Reinsch, F. M. Michel, C. Oumahi, G. V. Lowry and G. E. Brown Jr., Sulfidation processes of PVP-coated silver nanoparticles in aqueous solution: impact on dissolution rate, *Environ. Sci. Technol.*, 2011, **45**(12), 5260–5266.
31 J. Liu, K. G. Pennell and R. H. Hurt, Kinetics and mechanisms of nanosilver oxysulfidation, *Environ. Sci. Technol.*, 2011, **45**(17), 7345–7353.
32 O. Choi, T. E. Clevernger, B. Deng, R. Y. Surampalli, L. Ross Jr. and Z. Hu, Role of sulfide and ligand strength in controlling nanosilver toxicity, *Water Res.*, 2009, **43**(7), 1879–1886.
33 K. A. Huynh and K. L. Chen, Aggregation kinetics of citrate and polyvinylpyrrolidone coated silver nanoparticles in monovalent and divalent electrolyte solutions, *Environ. Sci. Technol.*, 2011, **45**, 5564–5571.
34 R. Ma, C. Levard, S. M. Marinakos, Y. Cheng, J. Liu, F. M. Michel, G. E. Brown Jr. and G. V. Lowry, Size-controlled dissolution of organic-coated silver nanoparticles, *Environ. Sci. Technol.*, 2011, **46**(2), 752–759.
35 T. Diedrich, A. Dybowska, J. Schott, E. Valsami-Jones and E. H. Oelkers, The Dissolution Rates of SiO2 Nanoparticles As a Function of Particle Size, *Environ. Sci. Technol.*, 2012, **46**(9), 4909–4915.
36 L. R. Pokhrel, B. Dubey and P. R. Scheuerman, Natural water chemistry (dissolved organic carbon, pH, and hardness) modulates colloidal stability, dissolution, and antimicrobial activity of citrate functionalized silver nanoparticles, *Environ. Sci.: Nano*, 2014, **1**, 45–54.
37 M. Baalousha, A. Manciulea, S. Cumberland, K. Kendall and J. R. Lead, Aggregation and surface properties of iron oxide nanoparticles: influence of pH and natural organic matter, *Environ. Toxicol. Chem.*, 2008, **27**(9), 1875–1882.
38 J. T. Siy and M. H. Bartl, Insights into Reversible Dissolution of Colloidal CdSe Nanocrystal Quantum Dots, *Chem. Mater.*, 2010, **22**(21), 5973–5982.
39 H. E. Pace, N. J. Rogers, C. Jarolimek, V. A. Coleman, E. P. Gray, C. P. Higgins and J. F. Ranville, Single particle inductively coupled plasma-mass spectrometry: A performance evaluation and method comparison in the determination of nanoparticle size, *Environ. Sci. Technol.*, 2012, **42**(22), 12272–12280.
40 R. Kaegi, A. Voegelin, C. Ort, B. Sinnet, B. Thalmann, J. Krismer, H. Hagendorfer, M. Elumelu and E. Mueller, Fate and transformation of silver nanoparticles in urban wastewater systems, *Water Res.*, 2013, **47**(12), 3866–3877.
41 D. M. Mitrano, A. Barber, A. Bednar, P. Westerhoff, C. Higgins and J. Ranville, Silver nanoparticle characterization using single particle ICP-MS (SP-ICP-MS) and asymmetrical flow field flow fractionation ICP-MS (AF4-ICP-MS), *J. Anal. At. Spectrom.*, 2012, **27**, 1131–1142.
42 D. M. Mitrano, E. K. Lesher, A. J. Bednar, J. Monserud, C. P. Higgins and J. F. Ranville, Detection of nano-Ag using single particle inductively coupled plasma mass spectrometry, *Environ. Toxicol. Chem.*, 2012, **31**, 115–121.
43 F. Laborda, J. Jimenez-Lamana, E. Bolea and J. R. Castillo, Selective identification, characterization and determination of dissolved silver (I) and silver nanoparticles based on single particle detection by inductively coupled plasma mass spectrometry, *J. Anal. At. Spectrom.*, 2011, **26**(7), 1362–1371.
44 C. Degueldre, P. Favarger and S. Wold, Gold colloid analysis by inductively coupled plasma-mass spectrometry in a single particle mode, *Anal. Chim. Acta*, 2006, **555**(2), 263–268.
45 R. Reed, C. P. Higgins, P. Westerhoff, S. Tadjiki and J. Ranville, Overcoming challenges in analysis of polydisperse metal-containing nanoparticles by single particle inductively coupled plasma mass spectrometry, *J. Anal. At. Spectrom.*, 2012, **27**, 1093–1100.
46 H. E. Pace, N. J. Rogers, C. Jarolimek, V. A. Coleman, C. P. Higgins and J. F. Ranville, Determining transport efficiency for the purpose of counting and sizing nanoparticles *via* single particle inductively coupled plasma mass spectrometry, *Anal. Chem.*, 2011, **83**(24), 9361–9369.
47 S. Hu, R. Liu, S. Zhang, Z. Huang, Z. Xing and X. Zhang, A new strategy for highly sensitive immunoassay based on single-particle mode detection by inductively coupled plasma

mass spectrometry, *J. Am. Soc. Mass Spectrom.*, 2009, **20**(6), 1096–1103.

48 L. Ebdon and A. Collier, Particle size effects on kaolin slurry analysis by inductively coupled plasma-atomic emission spectrometry, *Spectrochim. Acta, Part B*, 1988, **43**(4), 355–369.

49 Y.-J. Lee, J. Kim, J. Oh, S. Bae, S. Lee, I. S. Hong and S.-H. Kim, Ion-release kinetics and ecotoxicity effects of silver nanoparticles, *Environ. Toxicol. Chem.*, 2012, **31**(1), 155–159.

50 R. G. Miller, *Simultaneous statistical inference*, Springer, 1966, vol. 196.

51 J. Dobias and R. Bernier-Latmani, Silver release from silver nanoparticles in natural waters, *Environ. Sci. Technol.*, 2013, **47**(9), 4140–4146.

52 J. M. Gorham, R. I. MacCuspie, K. L. Klein, D. H. Fairbrother and R. D. Holbrook, UV-induced photochemical transformations of citrate-capped silver nanoparticle suspensions, *J. Nanopart. Res.*, 2012, **14**(10), 1–16.

53 C. M. Ho, S. K. W. Yau, C. N. Lok, M. H. So and C. M. Che, Oxidative dissolution of silver nanoparticles by biologically relevant oxidants: A kinetic and mechanistic study, *Chem.–Asian J.*, 2010, **5**(2), 285–293.

54 A. Bednar, A. Poda, D. Mitrano, A. Kennedy, E. P. Gray, J. F. Ranville, C. Hayes and F. Crocker, Comparison of On-Line Detectors for Field Flow Fractionation Analysis of Nanomaterials, *Talanta*, 2012, **104**, 140–148.

55 M. Delay, T. Dolt, A. Woellhaf, R. Sembritzki and F. H. Frimmel, Interactions and stability of silver nanoparticles in the aqueous phase: Influence of natural organic matter (NOM) and ionic strength, *J. Chromatogr. A*, 2011, **1218**(27), 4206–4212.

56 S. Diegoli, A. L. Manciulea, S. Begum, I. P. Jones, J. R. Lead and J. A. Preece, Interaction between manufactured gold nanoparticles and naturally occurring organic macromolecules, *Sci. Total Environ.*, 2008, **402**(1), 51–61.

57 C. Impellitteri, T. Scheckel and G. Kirk, The Speciation of Silver Nanoparticles in Antimicrobial Fabric Before and After Exposure to Hypochlorite/Detergent Solution, *J. Environ. Qual.*, 2009, **38**, 1528–1530.

58 J. Liu, D. A. Sonshine, S. Shervani and R. H. Hurt, Controlled release of biologically active silver from nanosilver surfaces, *ACS Nano*, 2010, **4**(11), 6903–6913.

59 R. Kaegi, A. Voegelin, C. Ort, B. Sinnet, B. Thalmann, J. Krismer, H. Hagendorfer, M. Elumelu and E. Mueller, Fate and transformation of silver nanoparticles in urban wastewater systems, *Water Res.*, 2013, **47**(12), 3866–3877.

60 M. Delay and F. H. Frimmel, Nanoparticles in aquatic systems, *Anal. Bioanal. Chem.*, 2012, **402**, 583–592.